Proceedings of DETC'97
1997 ASME Design Engineering Technical Conferences
September 14-17, 1997, Sacramento, California

DETC97/VIB-4255

GARTEUR GROUP ON GROUND VIBRATION TESTING — RESULTS FROM THE TEST OF A SINGLE STRUCTURE BY 12 LABORATORIES IN EUROPE

Etienne Balmès[1]
ONERA, Direction des Structures
B.P. 72
92322 Chatillon
France
balmes@onera.fr

Jan R. Wright
Dynamics and Controls Research Group
University of Manchester
Manchester, M13 9PL
United Kingdom
jrwright@fs1.eng.man.ac.uk

ABSTRACT

In an effort to assess state of the art methodologies for the experimental determination of modal characteristics, 12 European groups, most of them working in the area of aircraft ground vibration tests for flutter certification, participated in a GARTEUR action group whose main activity was to have independent tests of a single representative structure. Design considerations for the common structure are first detailed. Estimates of frequency response functions and modal characteristics are then compared and show a level of consistency that is much higher than those reported in previous similar exercises.

INTRODUCTION

In the certification of new aircraft, Ground Vibration Tests (GVT) play an important role for the verification or updating of analytical models, allowing more accurate aeroelastic predictions. Facing the risk of flutter, a high level of quality and reliability in obtaining the modal characteristics of the aircraft has to be achieved during the GVT.

Following a series of previous Round Robin surveys held in the early 60s (Remmers and Belsheim, 1964) and late 70s (Ewins and Griffin, 1981), a Structures and Materials Action Group SM-AG-19 of GARTEUR (Group for Aeronautical Research and Technology in Europe) was initiated in April 1995 with the major objective to compare a number of current measurement and identification techniques applied to a common structure. The testbed (see figure 1) was designed and manufactured by ONERA (France) and investigated by various companies, research centers and universities from France (ONERA, SOPEMEA, Aérospatiale, Intespace, CNAM), Germany (DLR), the Netherlands (NLR, Fokker), Sweden (Saab) and the United Kingdom (DRA, Manchester University, Imperial College).

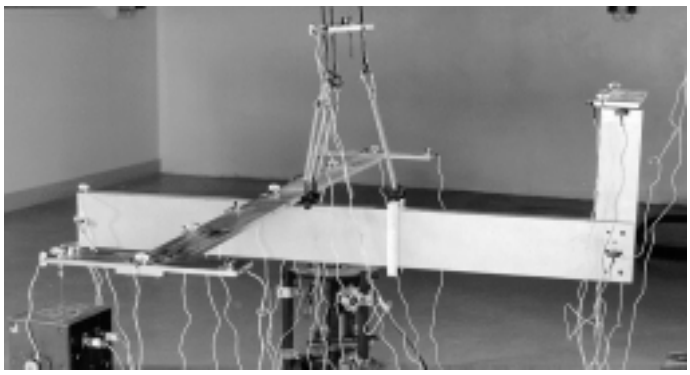

Figure 1. Common testbed of the GARTEUR SM-AG-19

More specifically, the objectives of the GVT tests were to evaluate the efficiency and reliability of test methods and to identify the cause of discrepancies between measured frequency responses or identified modal parameters. Each participant was required to provide:

- a set of 4 transfer functions corresponding to excitation and response of the left and right wing tip bodies (called

[1]This author receives the correspondence concerning this paper

drums in the rest of the paper) in the 4-60 Hz band. Although not required, most participants provided a 2 input 24 output set of transfer functions.
- estimated modal parameters (modeshape, frequency, damping factor, and modal mass) at 24 reference accelerometer locations.

The present paper outlines the activity of SM-AG-19 and compares data provided by the participants. Design considerations for the testbed and general comments on how the tests were performed are first outlined. Comparisons of the variability of results for frequency response functions, frequencies, damping ratios, modeshapes and mass normalized modes are then detailed.

In the comparisons, participants are identified by letters in chronological testing order. Data sets *DK* were obtained in a configuration differing from the test guidelines (see discussion on mass in previous section) are not comparable and are thus not included. Participant *L* performed the test but was unable to continue his participation in the exercise. Participant *H* did not provide frequency response functions and gave four estimates four each mode without proper selection of a best answer and no proper mass scaling. Participants *BJ* provided complex modes with a significant phase spread so that the modal mass estimates could not be found for their data.

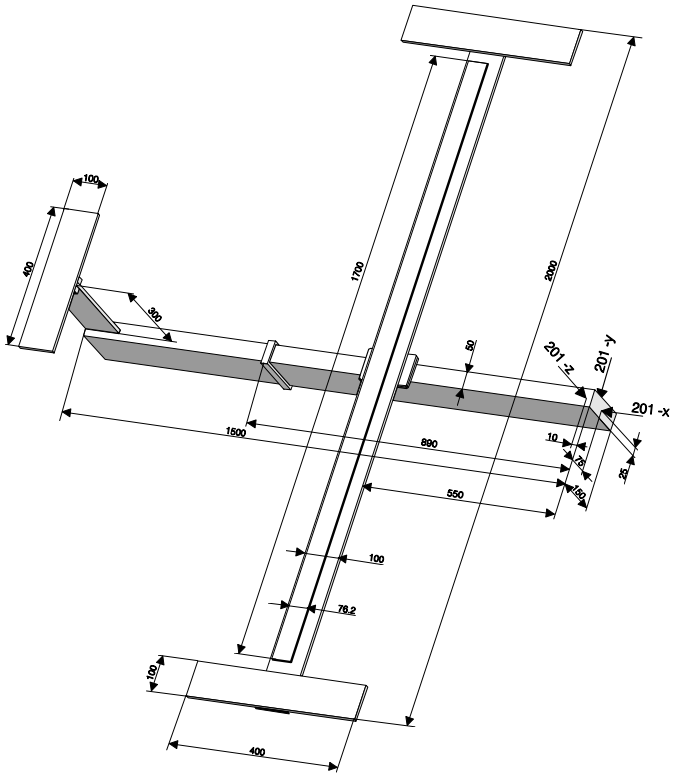

Figure 2. Testbed design.

TESTBED DESIGN

Specifications for the testbed were

- a group of 3 very close modes to make the problem difficult.
- 5 to 60 Hz, 50-100 kg, 2 by 2 m to make the testbed suitable for instrumentation designed for aircraft.
- a joint at the wing/fuselage connection for transportation but limiting variability from assembly to assembly.
- damping treatment to limit the effect of dissipation linked to instrumentation.
- suspension by a common set of bungees to have similar boundary conditions.
- 24 common sensor and 2 common shaker locations to allow direct comparisons.

The final design of the testbed as shown in figure 2 had a fuselage length of $1.5m$ and a wingspan of $2m$. The total mass was $44kg$.

The most difficult design criterion was the presence of 3 very close modes. On such a simple structure, close modal spacing can only be achieved by using modes of a different nature (bending modes in different directions, torsion modes, wing modes vs. tail modes). The relatively massive fuselage induces a near decoupling of torsion modes for each half wing, so that the first two torsion modes come as a pair. The design thus mostly adjusted the drum mass to put the frequency of the 2 torsions close to another mode (the 3 node bending eventually). As shown in figure 3, Nyquist plots of the final testbed show, near the resonance, a single lobe or three very coupled circles depending on the sensor.

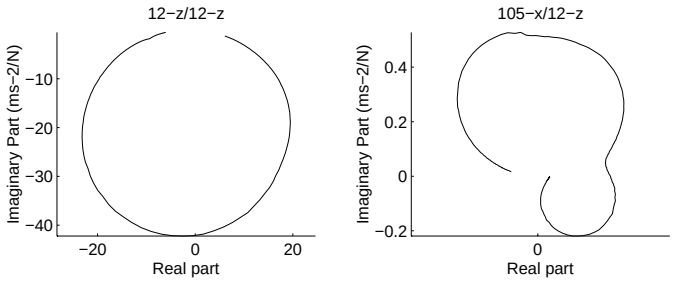

Figure 3. Nyquist plots near the resonance. A single circle is found on some transfer functions while the three modes are always very coupled.

To measure force, participants used load cells or electrical impedance (force/current factor on a current driven

shaker). With the second technique, the moving mass, stiffness and damping of the shaker becomes part of the measured structure. On an aircraft the moving masses are so small that the effect is negligible, but for this small testbed a way to compensate for the added mass was needed. The design thus placed a 200g compensation mass at each drum tip (as shown in Fig. 4). In a case where additional mass was known to be added, the nominal mass could thus be replaced by a smaller one to physically compensate for the effect (the fact that the mass position does not exactly coincide with the expected shaker position was not taken into account).

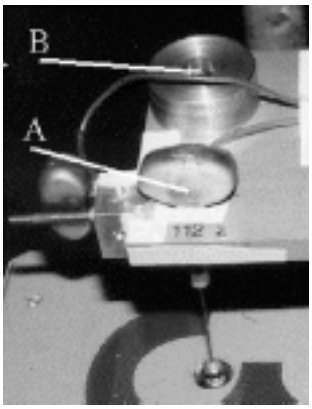

Figure 4. Shaker attachments on the axes of the accelerometer (A) or the compensation mass (B).

Figure 5 shows the sensitivity to tip mass removal. It clearly appears that the torsion modes undergo a significant frequency shift (39 to 33.5 Hz) while the frequency of the three node bending mode stays close to 35.6 Hz. This selective sensitivity significantly helped the design but was also one of the major sources of variations in the results of different tests. Inappropriate mass compensation was used for some tests so that not all data sets could be included in the comparisons of the following sections (sets DH are not included, set B is comparable but identified properties are significantly affected).

Some groups also positioned their shaker on the mass axis rather than on the accelerometer axis (positions A and B in figure 4) which resulted in significantly different results (see figure 9).

Sufficient damping levels were obtained through the use of a viscoelastic layer with an aluminum constraining layer (see figure 2). The viscoelastic used is the 3M acrylic viscoelastic polymer ISD 112 in the form of a $76.2mm$ by $50\mu m$

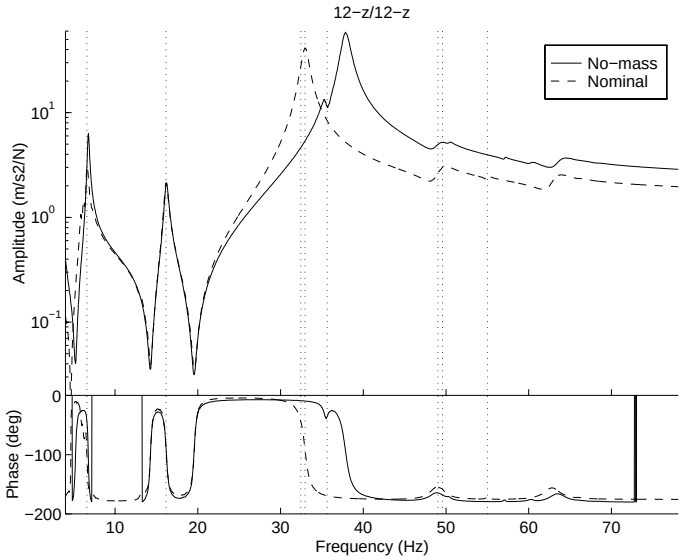

Figure 5. Sensitivity of FRFs to removal of the 200g tip masses.

roll. A sample roll (Ref: SJ 2015 Type 1202) was provided by 3M Laboratories (Europe), Hansastr. 9, 41453 Neuss, Germany. This viscoelastic is particularly well suited for the testbed operating range of $5 - 50Hz$ and $20°C$ where the loss factor is near its peak of 0.9.

Significant levels of shear strain are obtained in the viscoelastic through the use of a 1.1 x 76.2 x 170 mm constraining layer covering the complete viscoelastic treatment. The ISD 112 being pressure sensitive, the bonding was obtained easily and 3M confirmed that only extreme conditions should damage it. In a wing only test, damping factors increased significantly (from 0.28% to 1.1% in bending at 9 Hz and from 0.15% to 0.86% in torsion at 27 Hz) with the added treatment. Tests done on different days gave very similar results.

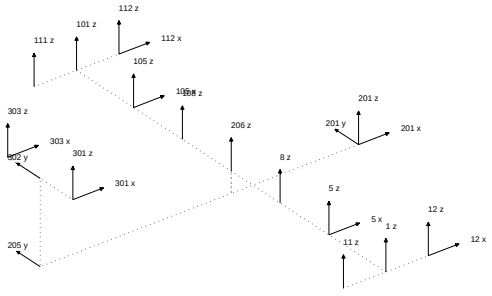

Figure 6. 24 common accelerometer locations. Nominal excitation locations are 12-z and 112-z.

The common 24 sensor locations, shown in figure 6, were chosen by hand early in the design process. As shown in table 1 by the off-diagonal terms of the Modal Assurance Criterion (MAC (Avitabile et al., 1988)) comparison of an experimental mode set with itself, this set of sensors has problems distinguishing mode pairs 1-6, 3-5 and 5-7. The fact that modes 3-5 are very close in frequency is an additional difficulty. No simple weighting of the sensors seems to significantly improve the geometric independence of these three mode pairs.

Table 1. Check of the sensor placement using the MAC comparison of a set of experimental modes with themselves.

#	1	2	3	4	5	6	7	8
1	100.	0.0	0.2	1.6	0.5	18.1	0.0	0.1
2	0.0	100.	0.5	0.2	0.0	0.1	0.1	0.0
3	0.2	0.5	100.	0.3	11.8	1.7	0.5	0.1
4	1.6	0.2	0.3	100.	1.1	1.8	0.1	2.0
5	0.5	0.0	**11.8**	1.1	100.	0.8	21.3	0.0
6	**18.1**	0.1	1.7	1.8	0.8	100.	0.5	0.4
7	0.0	0.1	0.5	0.1	**21.3**	0.5	100.	0.4
8	0.1	0.0	0.1	2.0	0.0	0.4	0.4	100.

Figure 7 shows the 9 modeshapes measured by participant C. The second mode was used as a check of proper assembly. As will be shown in the next sections, it was effectively the most consistently estimated mode. A posteriori, it should be said that this choice was not ideal since this mode was among the least sensitive to perturbations and thus not informative on the fact that the test configuration specification was met.

For all tests, the structure was suspended using bungees linked to a small plate common to all the participants (visible in figure 1). The participants were however free to attach the plate in any appropriate manner. Some fixed the plate to a hard point while others used pendulums of various lengths. Table 2 shows no direct relation between pendulum length and estimated rigid body heave mode.

Table 2. Length of suspension pendulum (length of bungees not included) and estimated frequency of heave mode.

Set	B	C	E-F	G	H	I	J
Length (m)	12.0	0.0	2.6	0.5	0.4	0.5	0.2
Freq (Hz)	1.9	1.8	2.7	2.2	2.6	2.4	2.0

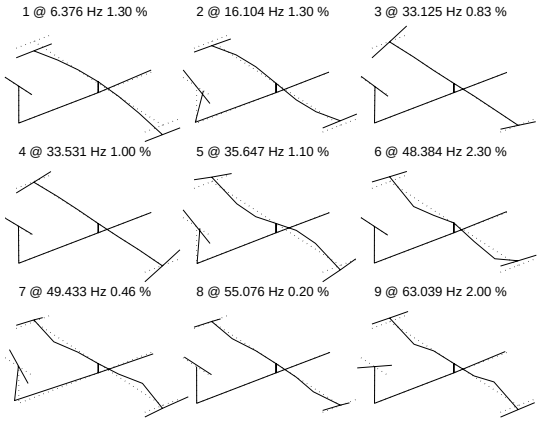

Figure 7. Set of modes measured by participant C.

COMPARISON OF MEASURED FRF

The participants were required to provide a 2 by 2 set of transfer functions with 2 collocated transfers (point mobilities) at the drum tips (12z and 112z) and 2 cross transfers (12z to 112z, 112z to 12z). The collocated transfers are expected to be equal because of the symmetry of the structure, and the cross transfers because of reciprocity.

Figure 8 shows a comparison of the 112z collocated transfers measured by a number of participants. General trends are clearly common to all measurements. Above 40 Hz, the response is however dominated by modes near 34 Hz so that it is hard to see how coherent the measurements are. Tests B and J show significant discrepancy near 35 Hz, these are however easily explained by the selection of inappropriate compensation masses.

The collocated transfers 12z are slightly different from those of figure 8 because the structure is not really symmetric (see details in the section on modeshape comparisons), but otherwise show little more information.

The required cross transfers (12z to 112z shown in figure 9) are much more informative. Some data sets are very noisy and/or show quantization errors. Data set A has for example a fairly high noise floor, which masks the anti-resonances of cross transfers. It must be noted however that the groups who provided noisy data sets do not use FRF data for identification purposes.

Resonance frequencies show significant variability from test to test. For example, the resonance of the first mode goes from 6.4 to 7 Hz. These variations are coherent with the modal results given by the participants. Despite frequency shifts, the general trends (positions of resonances

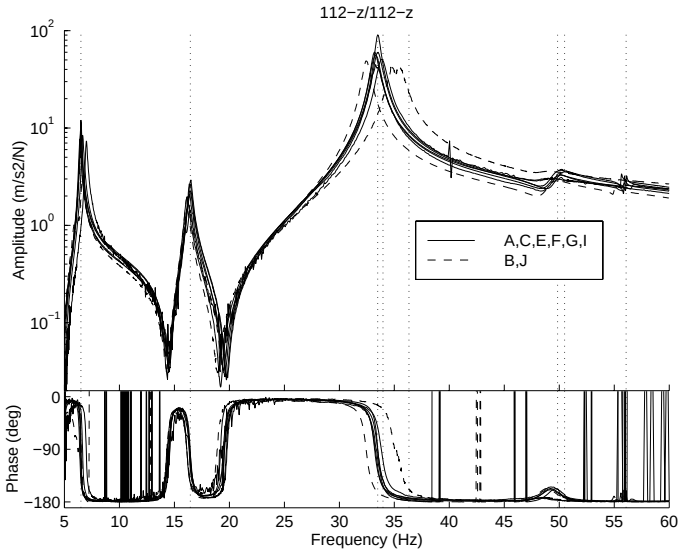

Figure 8. Collocated transfer function at left drum (112z).

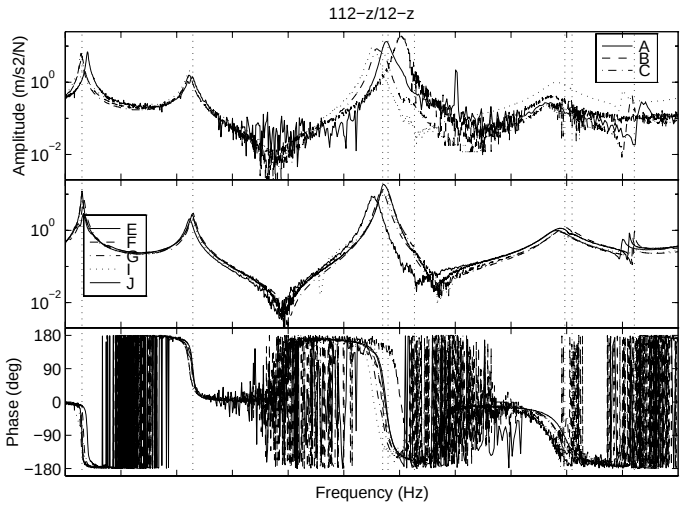

Figure 9. Cross transfer 112z to 12z. Amplitude plots are separated in two groups depending on shaker position (A and B in figure 4).

and anti-resonances) are well preserved in all data sets. Sets B and J have again the resonances of the torsion modes shifted up and down respectively.

Figure 9 distinguishes sets ABC from sets $EFGJ$ based on where the shaker was attached (positions A and B of figure 4). Above 35 Hz, the two sets show a significant difference in the level of response. Within each set, the responses are however coherent.

Figure 10a and 10b show transfers between drum excitation and the in plane mid-wing sensor. Sets A,C which are very noisy for these sensors have been removed. Sets B,J are shown in dotted lines and one sees the frequency shifts near 35 Hz. Set J significantly differs from other sets which may account for the discrepancies seen for modeshapes (see the following sections).

Sensors 5x, 105x and sensor 201x even more (figure 10c) indicate the presence of many suspension modes in the 5-15 Hz range. These modes are hardly seen in the response of vertical sensors except for group J which was unlucky enough to have the frequency of 2 suspension modes coincide with the 2 node bending mode.

Drops in the second Mode Indicator Function of figure 10d clearly indicate the presence of the two torsions (33.8 Hz) and tail torsion (49.4 Hz). The 3 node bending (35.7 Hz) is however not very well excited (the minimum of the MIF is above 0.8) which shows that these shaker positions are not suited for a force appropriation of this mode (participant H limited himself to this shaker configuration).

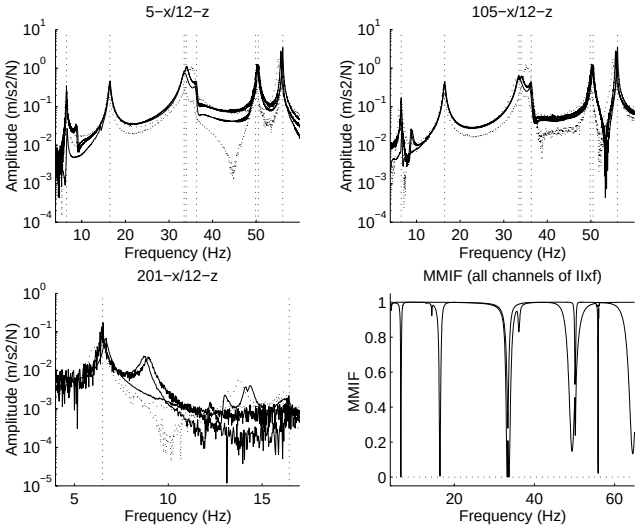

Figure 10. a-b: cross transfers 12z to 5x and 105x. c: low frequency range of 201x/12z. d: Multivariate Mode Indicator Function (Williams et al., 1985) for inputs 12z and 112z.

One should also note that the force measurement technique (groups ACG use current driven amplifiers, others use load cells) or the input signal used (participants used stabilized and swept sine, single and multiple input broadband signals) do not appear to have any significant influence. Noise levels seem to be inversely proportional to how much they were used for identification purposes. Even for groups using identification, responses to non reference inputs were used to identify some modes (3 node bending

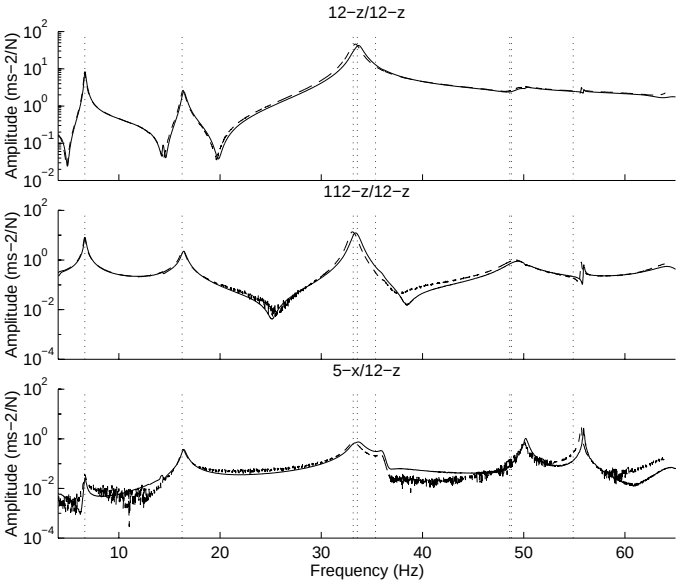

Figure 11. Comparison of two tests performed by ONERA.

and in plane modes in particular).

As a check for the variability of results, the test was performed at ONERA in the middle and the end of the testing period. The two tests differ by shaker stinger, shaker suspension, testbed bungees, excitation level. The results shown in figure 11 are thus a case where a marginal evolution of test conditions leads to visible differences in the test response. The change in noise level is related to a change in the algorithm used to detect stabilization in a stepped sine but shifts of resonance frequencies are clearly apparent. It is not possible to tell whether these are due to modifications of the structure or of the test set-up but they are significant and of the same order as variations seen between results of different participants. Further tests will be performed to clarify this issue.

COMPARISON OF FREQUENCIES AND DAMPING

The second part of the exercise was to provide estimates of modal characteristics: frequency, damping ratio, modeshape and modal mass. Participants *ACEGH* provided results obtained using force appropriation method, while other results are based on model identification from measured transfer functions. The results shown do not indicate any influence of the method used on the results obtained.

Figure 12 shows the typical spread of identified modal frequencies to be close to 4 %. Many frequency discrepancies can be related to structural modifications linked to the

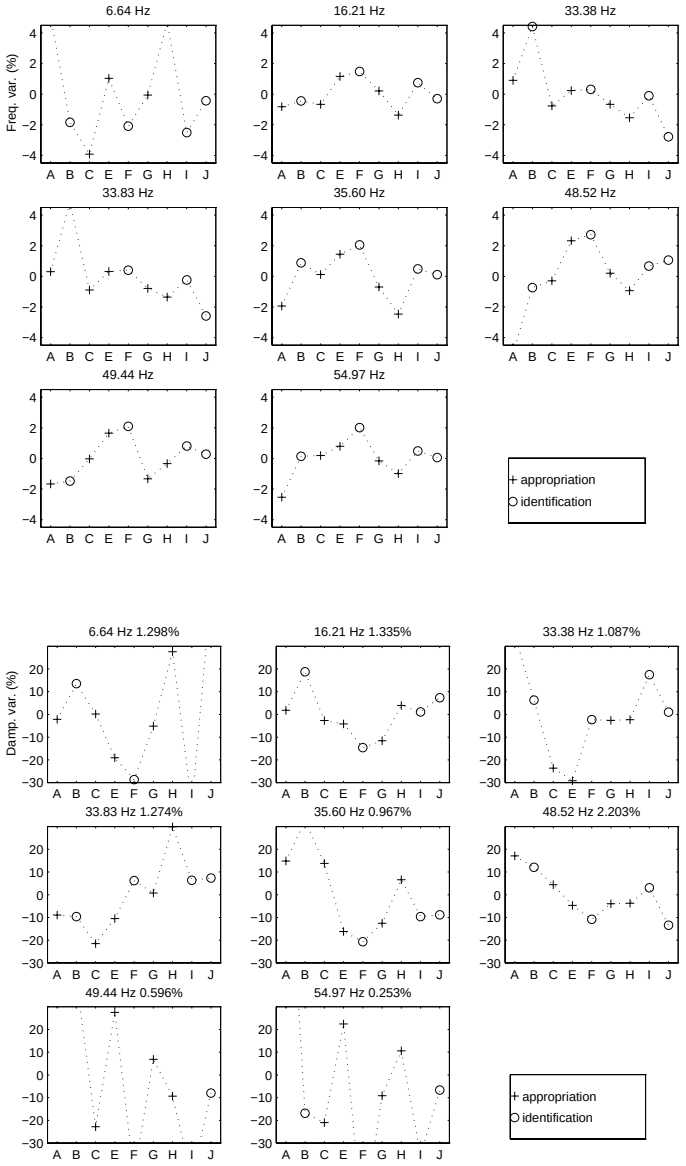

Figure 12. Variations in estimated modal frequencies and damping ratios. Mean values given in the titles.

instrumentation or selection of compensation masses. For example, an insufficient compensation mass leads for test *B* to the high frequency estimate of the 2 torsion modes (33.45 and 33.89 Hz). However, no simple explanation of the high variability of frequency estimates for mode 1 was found.

For damping ratios, the typical spread is closer to 30%. Modes 7 and 8 show the highest variations but also have the lowest damping values. This only confirms the fact that very lightly damped modes are difficult to characterize. In

particular, instrumentation is likely to contribute most of their damping so that one should not expect their damping values to stay constant. This expected sensitivity was the main reason to design a damping treatment to increase the overall damping of the testbed.

Another question of interest is the sensitivity of the results to the method used. The plots do not indicate any particular trend that would be characteristic of either identification or force appropriation. To confirm that the variability of results is indeed linked to changes in the structure/test setup and not the method, the IDRC (Balmès, 1996) identification method was used on available data sets to provide independent estimates of modal frequencies.

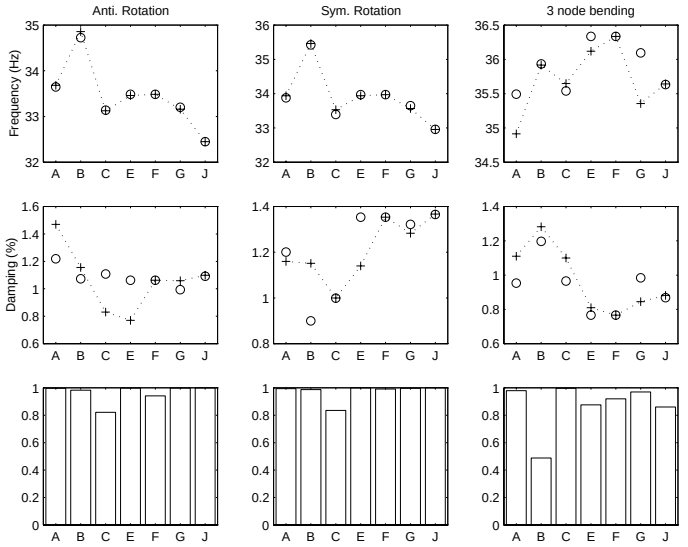

Figure 13. Comparison of the 3 close modes given by the groups with results independently identified from their FRF data (IDRC method).

For the three close modes, figure 13 shows that the only visible frequency variations from the participants results are found for the 3 node bending for groups *ACEG*. These groups used force appropriation and good appropriation of the 3 node bending cannot be achieved with the drum tip shakers only. These groups thus had to use another shaker and, given the modification of the test setup, variations of frequencies are expected. Group *C*, who attached the shaker to the fuselage, minimized this effect and the frequency difference is low. The FRFs of this group to the 2 reference inputs are not however consistent (resonance frequencies shift when the input is changed). The identification was thus performed on a single excitation which may explain the relatively poor MAC comparison of torsion modeshapes. On real aircraft, dependence on input location is often linked to the presence of non linearities. On the considered testbed it is more likely that the instrument loading changed between tests.

COMPARISON OF MODESHAPES

The participants were all asked to compare their results with those of test *A*. This test however happens to have rather different modes 4 and 5 so that set *C* will be used as reference here. The MAC comparisons shown in figure 14 indicate a very good overall correlation. The only MACs below 0.4 are mode 7 of set *F* and 8 set *H*) which are exceptional errors. Modes 3-5 have problems for sets *ABEH* which will be analyzed later on.

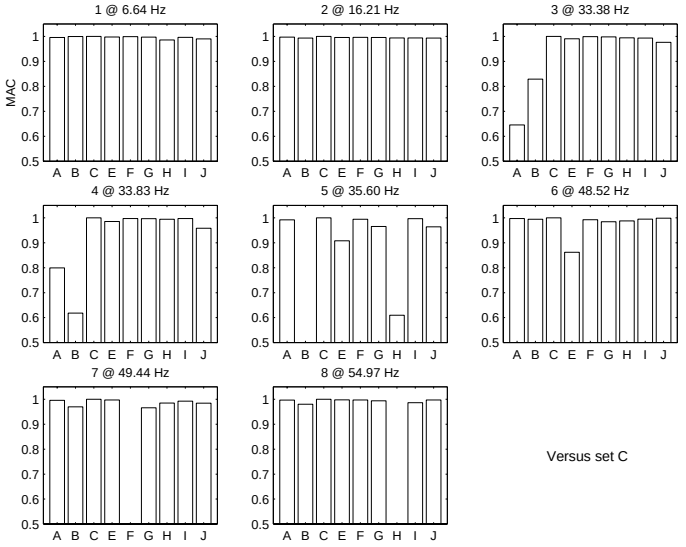

Figure 14. Diagonal MAC values for comparison of different test modeshapes with those of test *C*.

The MAC does not provide a perfect comparison of modeshapes. Figures 15-16 overlay the modes identified by the different participants. For this purpose all modal vectors shown in the figure are normalized to unity. As proposed in Degener (1997), the measurement points are arranged following the geometry of the testbed. The first five measurement points are the in-plane wing accelerometers. The next block of data shows the vertical wing motion including the drums. The remaining fuselage and tail accelerometers are plotted last.

Mode 1 and 2 (which served as a check) show extremely good correlation.

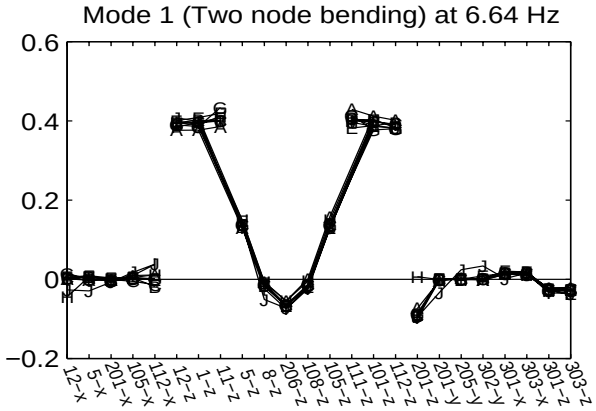

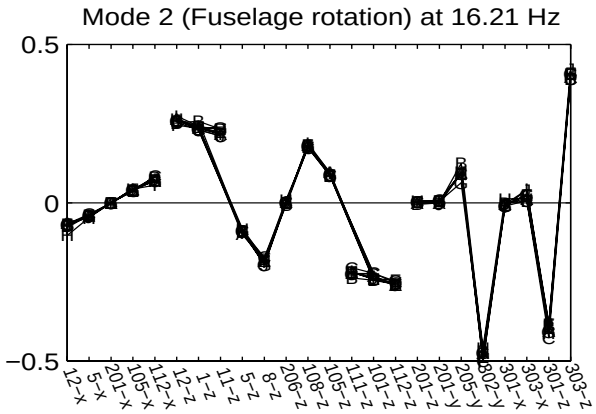

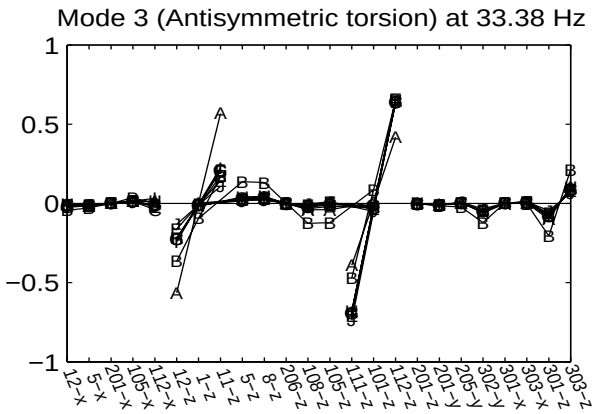

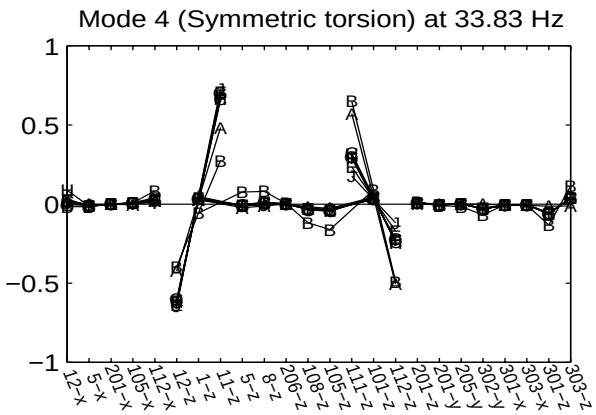

Figure 15. Measured modeshapes 1-4 normalized to unity

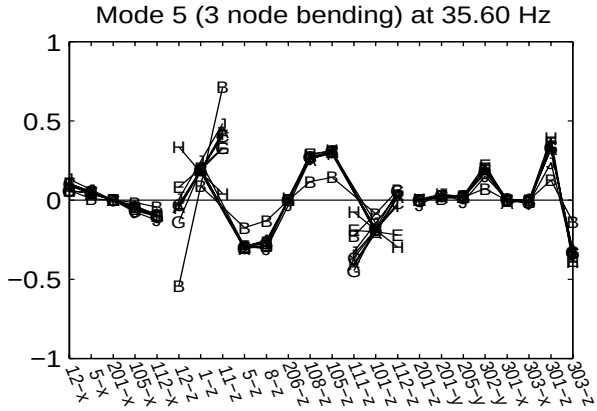

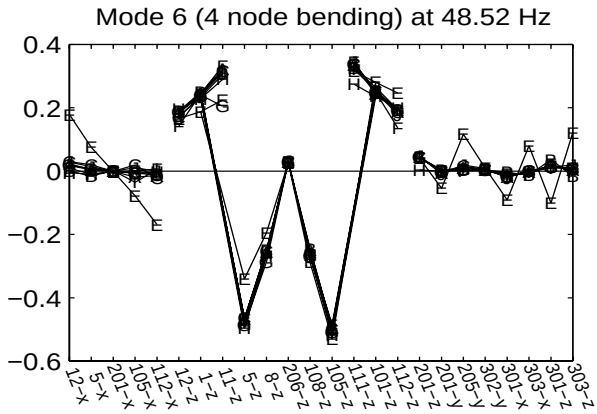

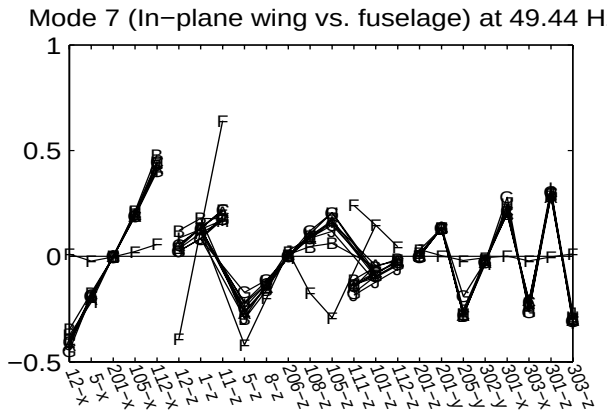

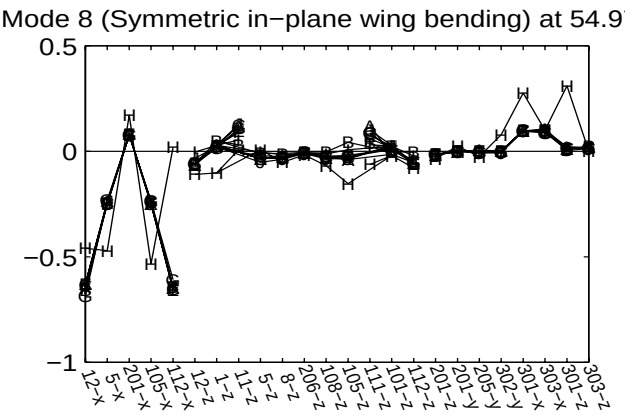

Figure 16. Measured modeshapes 5-8 normalized to unity

Mode 3, the 'antisymmetric torsion' mode, is the first of the three closely spaced modes. The wing structure is not truly symmetric ($1mm$ difference between the widths of the left and right sides), which leads to a significant dissymmetry of modeshapes which was measured consistently by 7 participants. The opposite effect was noted for mode 4, the 'symmetric torsion' mode. Participant A seems to have forced the symmetry and participant B is known to have chosen inappropriate compensation masses so that modes 3-5 are expected to be affected.

Mode 5, the fundamental 3 node bending, is closely spaced with the torsional modes. Although the vertical displacement patterns are similar, the bending/torsion coupling is not consistently identified (the sign found for sets EH is even different). Participant H actually provides 4 estimates of the modeshapes, the one kept for the database is the only one with an error on the torsion. Participant E appropriated mode 5 using vertical excitation at the drums. This selection of a force inputs does not allow good appropriation of this mode and the result should be taken with caution. In a flutter certification test, such limitations would be typically seen and additional shakers used.

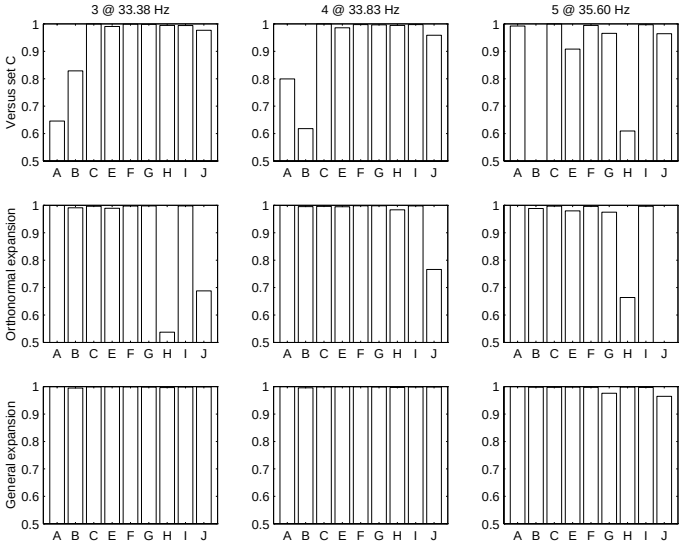

Figure 17. a) MAC comparison with test C, b) Comparison after orthonormal expansion, c) Comparison after general expansion.

It is well known that modes that are close in frequency can be very sensitive to small modifications of the structure. The symmetric and antisymmetric torsions (modes 3-4) and the 3 node bending (mode 5) are very sensitive to mass stiffness modifications. Since the instrumentation of each participant is expected to vary, non-negligible perturbations are expected. Such perturbations however will only induce recombination of modes that are close in frequency (this is the case of modes 3-5). It could be further argued that the recombination should be almost orthogonal since orthogonality conditions always exist even for modes with equal frequencies.

A general linear combination and an orthogonal linear combination of the basis of the modeshapes 3-5 is done to improve the match between each set and set C. The resulting comparison of modeshapes (shown in Fig. 17) shows a very significant improvement over the results of Fig. 14. Even for the orthonormal expansion, only sets H and J have difficulties which may be explained by a poor normalization of the results given by these groups (which could not be included in the comparison of mass normalized modeshapes in the next section).

MODAL MASSES AND FRF PREDICTIONS

Modal masses are the last step of the comparison. The classical approach is to select a sensor for each mode (typically the one with the maximum response) and to compare the modal masses obtained by the different participants. To lower the sensitivity to the choice of a particular sensor, one will also consider a Modal Scale Factor defined as follows. Modeshapes are mass normalized so that the reconstructed FRF are given by

$$H_{kl} = \sum_{j=1}^{N} \frac{(c_k \phi_j)(\phi_j^T b_l)}{s^2 + 2\zeta_j \omega_j s + \omega_j^2} \tag{1}$$

where b, c are used here to represent the extraction of the proper component of the measured modeshape. The modal scale factor f given by

$$f_{AB} = \frac{(c_k \phi_j)^T_{\text{Test A}} (c_k \phi_j)_{\text{Test B}}}{(c_k \phi_j)^T_{\text{Test A}} (c_k \phi_j)_{\text{Test A}}} \tag{2}$$

is the coefficient by which scaled test mode $(c_k \phi_j)_{\text{A}}$ should be multiplied to minimize its difference with $(c_k \phi_j)_{\text{B}}$. If the modeshapes are identical, this coefficient is a direct indication of the error on the scaling (and thus on the modal mass).

Table 3 shows compares sets $AEFGI$ to the results of set C (proper scaling of other mode sets is not available). The comparison is only appropriate if the modeshapes are similar, so that scale factors corresponding to low MAC

Table 3. Comparisons of modal masses provided by different groups. a) relative error (in %) with respect to set C of modal mass at point of maximum response. b) modal scale factors (difference to 1 in %) with respect to set C.

	1	2	3	4	5	6	7	8
Hz	6.38	16.10	33.12	33.53	35.65	48.38	49.43	55.08
	111z	302y	111z	11z	11z	105z	112x	112x
C	4.50	4.30	0.78	0.82	4.50	2.70	7.20	4.30
a)								
A	5	-22	-69	-55	29	-13	-21	-10
E	5	5	16	14	-24	9	20	-30
F	5	17	13	24	28	37	-100	11
G	11	-17	-1	25	-30	-2	-25	-15
I	323	50	-14	-4	-6	-40	-49	-32
b)								
A	-3	-7	-21	-17	7	-6	-6	-4
E	9	5	5	0	2	-8	10	-17
F	3	8	6	7	12	20	-96	7
G	3	-4	0	6	3	-3	-6	-1
I	109	29	-7	-4	-5	-21	-23	-18

values are shown in small characters in the table and should not be considered for the comparison.

The comparison at the point of maximum response shows significant differences while the modal scale factor indicates very good correlation. It is an open discussion to know which indication of error should be retained.

Most identification methods tend to preserve the response at resonance ($s = i\omega$). From (1), an error on the damping ratio would thus tend to be compensated by an error in the same direction on the modal mass. It is particularly interesting to note that the damping variations (shown in figure 12) are much more significant than the modal scale factor variations so that they cannot be attributed to bad identification. It seems that damping changed from test to test, while modal mass was properly identified and was, as expected, independent of the damping level.

One can again try to see if the results found depend on the parameter extraction method used. For mode 2, the IDRC identification algorithm was again used on data sets EFGJ. The resulting mass normalized modeshape is shown in figure 18 where only very minor variations are seen (the error on sensor 20 group E is just a calibration problem). For sets ABC, the results are also very similar except for a

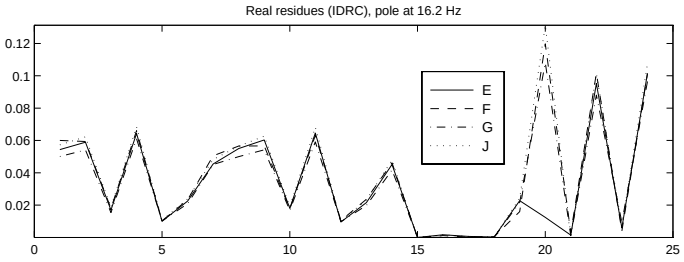

Figure 18. Mass normalized shape of mode 2 found by IDRC identification using different data sets.

scale factor of about 1.05. This difference is easily explained by the fact that these groups excited at point B (see figure 4).

As a final quality check FRF were generated from the identified modal quantities and are shown in figure 19. These predictions only take 8 modes into account. The contribution of mode 9 (65 Hz) and higher modes are not negligible and account for some of the visible discrepancies between the synthesized and test FRFs. Exceptional errors (modeshape 7 for set F, scaling error on mode 1 for set I) lead to poor predictions of many FRFs. Significant frequency shifts for modes 1,6 and 8 of test A and discrepancies for modes 5 and 6 of test E deteriorate the predictions of these two tests. Finally, sets C and G compare extremely well on most FRFs (in the third FRF of of figure 19, mode 5 sensor 12z is important which accounts for the notable differences in the antiresonances above 25 Hz).

CONCLUSIONS

Although the methods and hardware used by different participants were widely different, the results compare very well. Force measurement techniques through load cell or current measurements did not lead to any visible modification of the frequency responses.

Force appropriation and identification methods led to very similar modeshape estimates. Identification results were however generally given as complex modes. Simple methods were used to determine normal modes but vector normalization was sometimes lost in this process. Variability in frequencies were of the order of 4%, in damping of the order of 30%.

No agreement was found on a proper measure of variability in estimated modal masses. When using the modal scale factor, discrepancies were found to be below 10% which is significantly below the 30% found for damping ratios. This leads to think that damping truly varied significantly from test to test while participants were able to properly identify mass normalized modeshapes.

The force appropriation of certain modes implies the use of additional shakers which, for this small testbed, introduces modifications linked to instrument loading. The testbed is mostly linear, has only one difficulty with closely spaced modes and uses a small number of sensors. None of the main reasons that make force appropriation useful are met. The results still compare extremely well.

Many of the important variations between the various test results could be traced back to inappropriate mass compensation of the shaker moving mass, or mass and stiffness loading of the structure by instruments or suspension. For tests performed a year apart by the same team, visible variations were found without having the possibility to determine if these were due to changes in the structure or the test conditions. This highlights the difficulty of obtaining the desired test conditions or simply characterizing the effect of the actual instrumentation.

Future group activities will be to compare identification results on a common data set, in an exercise similar to the SVIB Round Robin (Ahlin, 1996) but based on actual test data, and to analyze strategies considered for shaker and sensor placement.

REFERENCES

Ahlin, K., "Round Robin Exercise on Modal Parameter Extraction," IMAC, 1996, pp.273-277

Avitabile, P., O'Callahan, J., Milani, J., "Model Correlation and Orthogonality Criteria," IMAC, 1988, pp. 1039-1047

Balmès, E., 1996, "Frequency domain identification of structural dynamics using the pole/residue parametrization," IMAC, pp. 540-546

Degener, M., 1997, "Ground Vibration Tests on an aircraft model performed as part of a European Round Robin exercise," Aeroelasticity Forum, Rome

Ewins, D.J., Griffin, J., 1981, "A State of the Art Assessment of Mobility Measurement Techniques - Results for the Mid-Range Structures (30-3000 Hz)," Journal of Sound and Vibration, 78-2, pp. 197-222

Remmers, G.M., Belsheim, R.O., 1964 "Effects of technique on reliability of mechanical impedance measurement," Shock and Vibration Bulletin, 34-3

Williams, R., Crowley, J., Vold, H., 1985, "The Multivariate Mode Indicator Function in Modal Analysis," IMAC, pp. 66-70

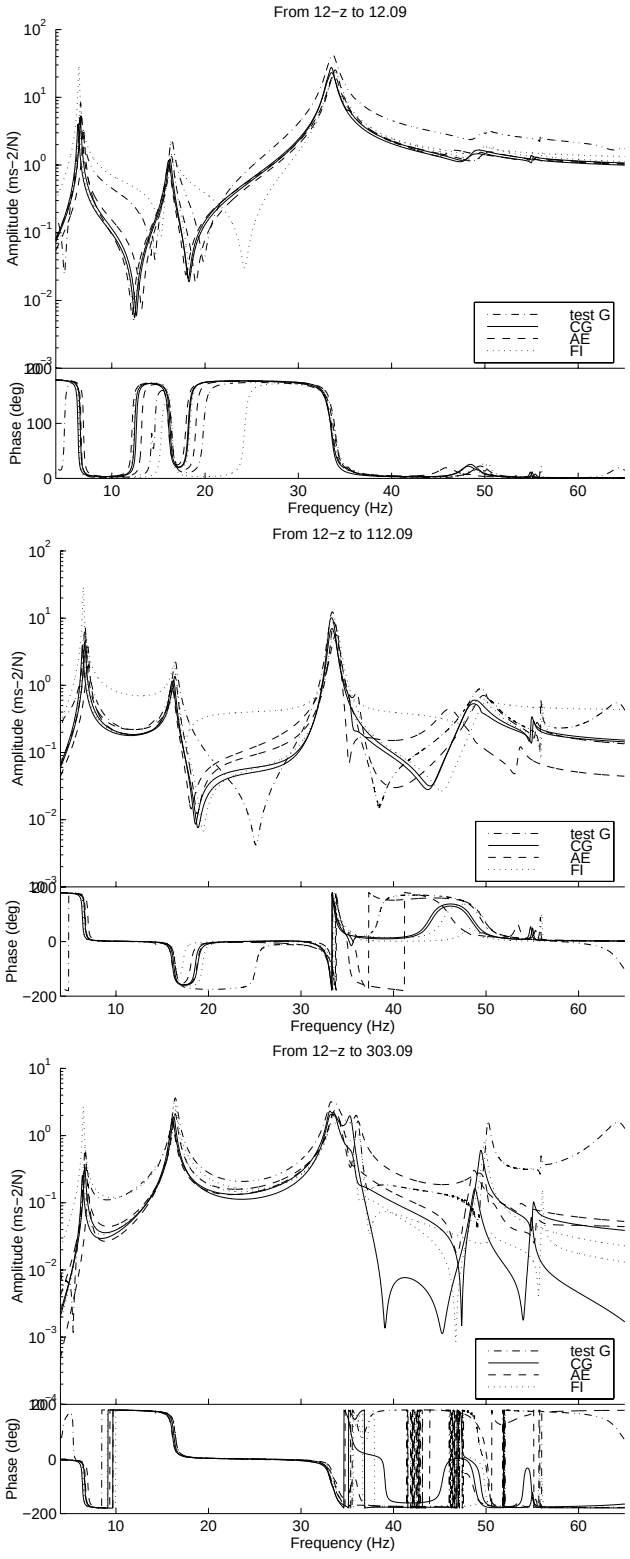

Figure 19. 3 FRF predictions based on the 8 provided mass normalized modes (sets $ACEFGI$). Solid line is measurement from G.